Astron. Astrophys. 344, 721–734 (1999)

ASTRONOMY AND ASTROPHYSICS

Gravitational lensing statistics with extragalactic surveys

I. A lower limit on the cosmological constant

Ralf Quast[1] **and Phillip Helbig**[2]

[1] Universität Hamburg, Hamburger Sternwarte, Gojenbergsweg 112, D-21029 Hamburg, Germany
[2] University of Manchester, Nuffield Radio Astronomy Laboratories, Jodrell Bank, Macclesfield, Cheshire SK11 9DL, England

Received 2 December 1998 / Accepted 14 January 1999

Abstract. We reanalyse optical gravitational lens surveys from the literature in order to determine relative probabilities in the λ_0-Ω_0 plane, using a softened singular isothermal sphere lens model. In addition, we examine a portion of the λ_0-Ω_0 plane which includes all viable cosmological models; this is vital for comparison with other cosmological tests. The results are, within the errors, consistent with those of more specialised analyses, such as those concerning upper limits on λ_0 in a flat universe. We note that gravitational lensing statistics can provide a quite robust *lower* limit on the cosmological constant as well, which could prove important in confirming current claims of a positive cosmological constant. At 95% confidence, our lower and upper limits on $\lambda_0 - \Omega_0$, using lens statistics information alone, are respectively -3.17 and 0.3. For a flat universe, these correspond to lower and upper limits on λ_0 of respectively -1.09 and 0.65.

Key words: cosmology: observations – cosmology: theory – cosmology: gravitational lensing

1. Introduction

The use of gravitational lensing statistics as a cosmological tool was first considered in detail by Turner et al. (1984); the influence of the cosmological constant was investigated thoroughly by Fukugita et al. (1992), building on the work of Turner (1990) and Fukugita et al. (1990). More recently, Kochanek (1996, hereafter K96, and references therein) and Falco et al. (1998) have laid the groundwork for using gravitational lensing statistics for the detailed analysis of extragalactic surveys. However, these analyses either have concentrated on a small subset of the possible cosmological models as described by the density parameter Ω_0 and the cosmological constant λ_0, have used a simpler (singular) lens model or both. This analysis is the first time λ_0 and Ω_0 have been used as independent parameters in conjunction with a non-singular lens model in an analysis of this type, complementing similar analyses with other emphases. (See Cheng & Krauss (1999) for a discussion of the importance of including a core radius.) Also, we include enough of the λ_0-Ω_0 plane to avoid neglecting any possibly viable models; this also makes the comparison with a variety of other cosmological tests easier. This is especially important in light of the fact that many analyses (e.g. Perlmutter et al. 1998; Riess et al. 1998; Schmidt et al. 1998; Carlberg et al. 1998a; Lineweaver 1998; Guerra et al. 1998; Daly et al. 1998) are now suggesting that our universe may contain a significant cosmological constant *and* be non-flat.

The plan of this paper is as follows. Sect. 2 reviews the groundwork and serves to define our notation. In Sect. 3 we specify the observational data and selection functions we use and formulate prior information about the parameters λ_0 and Ω_0. Sect. 4 describes the parametric submodels we use and the numerical computations we perform. In Sect. 5 we discuss our results and compare them with others. Sect. 6 presents our summary and conclusions.

2. Probability of multiply imaged sources

In this section we briefly review the statistical concepts introduced in K96; this also serves to define our notation. Note that with regard to cosmogical notation we follow that of Kayser et al. (1997), repeating here only 2 equations needed for discussion in this paper: the comoving spherical volume element at redshift z reads

$$\mathrm{d}V = 4\pi r^2 \frac{c}{H_0} \frac{\mathrm{d}z}{\sqrt{Q(z)}}, \tag{1}$$

where

$$Q(z) = \Omega_0(1+z)^3 - (\Omega_0 + \lambda_0 - 1)(1+z)^2 + \lambda_0. \tag{2}$$

Following the K96 approach, we assume that the light deflection properties of the gravitational lenses can be modelled with a particular type of circularly symmetric lens models with a monotonically declining radial mass profile. Such lens models generally create three images and have two critical radii on which the magnification diverges (e.g. Schneider et al. 1992). It is possible to estimate the probability $p(m, z_\mathrm{s})$ of the event

> *A source at redshift z_s is triply imaged. The total apparent magnitude of the three images is m. The image*

Send offprint requests to: R. Quast
Correspondence to: rquast@hs.uni-hamburg.de

configuration meets the selection criteria S and, particularly, shows the properties C.

If the outer and inner critical angular radii of the lens potential are respectively r_+ and r_-, the image magnification at radial angular position r is $\mu(r)$, the total magnification of the three images of a source at angular position y is $M(y)$, the functions $S(y)$ and $C(y)$ are $0|1$ valued selection functions, the comoving density of lenses of luminosity L is $\mathrm{d}n/\mathrm{d}L$ and the number-magnitude counts of sources are $\mathrm{d}N/\mathrm{d}m$, then

$$p(m, z_\mathrm{s}) = \frac{1}{2}\int_0^{z_\mathrm{s}} \frac{\mathrm{d}V}{\mathrm{d}z} \int_0^{\infty} \frac{\mathrm{d}n}{\mathrm{d}L} \int_{r_-}^{r_+} r|\mu(r)|^{-1} \times \underbrace{B(m, z_\mathrm{s}, y)S(y)C(y)}\, \mathrm{d}r\, \mathrm{d}L\, \mathrm{d}z, \quad (3)$$

where

$$B(m, z, y) = \frac{\mathrm{d}N}{\mathrm{d}m}\{m + 2.5\log[M(y)], z\} \left[\frac{\mathrm{d}N}{\mathrm{d}m}(m, z)\right]^{-1}. \quad (4)$$

The critical radii, the image magnifications and the source position are functions of the lens model, the luminosity of the lens galaxy and the redshifts of the source and the lens galaxy. If the underbraced functions are dropped, Eq. (3) yields the optical depth – the fraction of the sky included within the caustics of all lenses between us and the sources at redshift z_s. The inclusion of these functions accounts for magnification bias, survey selection effects (including what is defined as a lensing event) and allows the observed image separation to be taken into account.

Eq. (3) parametrically depends on λ_0 and Ω_0 through Eq. (1) and through the angular size distances,[1] which are needed for calculating observable quantities from the lens model (these also depend on the source and lens redshifts). Eq. (3) additionally depends on parametric submodels required to model the lens population and the number-magnitude counts of sources. Since throughout this paper we are principally interested in λ_0 and Ω_0, hereafter we refer to the submodel parameters as nuisance parameters (although technically they are on the same footing with λ_0 and Ω_0, there are not of as much interest here and thus a nuisance). In principle, one could also incorporate other observables into the parametric model; the reasons for not doing so are practical.

Assuming the survey selection function S is known, we can numerically compute Eq. (3) and reasonably estimate the probability $1 - p(m_i, z_i)$ that the quasar i is singly imaged or the probability $p(m_i, z_i, \theta_i)$ that the quasar i is multiply imaged and its images (within some tolerance) are separated by θ_i. If the survey data D contains M singly and N multiply imaged quasars, we can estimate the probability of the event

In a model universe fixed by the cosmological parameters λ_0, Ω_0 and the nuisance parameters $\boldsymbol{\xi}$, a multiply imaged quasar survey collects the observational data D.

[1] In general, the angular size distances depend not only on λ_0 and Ω_0 but on the degree of homogeneity in the universe as well (see, e.g., Kayser et al. 1997). However, in contrast to some other cosmological tests, this effect is relatively unimportant for the type of analysis performed here (see, e.g., Fukugita et al. 1992).

by applying the parametric model (or likelihood function)

$$\ln[p(D|\Omega_0, \lambda_0, \boldsymbol{\xi})] = -\sum_{i=1}^{M} p(m_i, z_i) + \sum_{j=1}^{N} \ln[p(m_j, z_j, \theta_j)], \quad (5)$$

where the logarithm $\ln[1 - p(m_i, z_i)]$ was expanded to first order. We can combine surveys of different objects by adding the logarithms of the likelihood functions for the individual surveys, and can combine surveys containing the same objects by applying their joint selection function.

In Bayesian theory the model parameters λ_0, Ω_0, $\boldsymbol{\xi}$ are regarded as random quantities with known joint prior probability density function $p(\lambda_0, \Omega_0, \boldsymbol{\xi})$. Applying Bayes's theorem, the appropriate posterior probability distribution given the observational data D is

$$p(\lambda_0, \Omega_0\boldsymbol{\xi}|D) = p(D|\lambda_0, \Omega_0, \boldsymbol{\xi}) \otimes p(\lambda_0, \Omega_0, \boldsymbol{\xi}), \quad (6)$$

where the operation '$\otimes$' denotes multiplication followed by normalisation. Marginalising the nuisance parameters

$$p(\lambda_0, \Omega_0|D) = \int p(\lambda_0, \Omega_0, \boldsymbol{\xi}|D)\, \mathrm{d}\boldsymbol{\xi}. \quad (7)$$

yields the (marginal) posterior probability density function for the parameters λ_0 and Ω_0. In the limit where all nuisance parameters take a precise value, $\boldsymbol{\xi} = \boldsymbol{\xi}_0$, the joint prior probability density function $p(\lambda_0, \Omega_0, \boldsymbol{\xi})$ factorises into $p(\lambda_0, \Omega_0)$ and a delta distribution $\delta(\boldsymbol{\xi} - \boldsymbol{\xi}_0)$, and Eq. (7) simplifies to

$$p(\lambda_0, \Omega_0|D) = p(D|\lambda_0, \Omega_0, \boldsymbol{\xi}_0) \otimes p(\lambda_0, \Omega_0). \quad (8)$$

On the basis of Eq. (7) or Eq. (8), we can calculate confidence regions for two parameters or perform further marginalisations and calculate mean values, standard deviations and marginal confidence intervals for one parameter.

3. Observational data and prior information

We use the observational data of the optical multiply imaged quasar surveys by Crampton et al. (1992), Jaunsen et al. (1995), Kochanek et al. (1995), Yee et al. (1993) and the observational data of the HST Snapshot Survey compiled by Maoz et al. (1993), including Q 0142-100, Q 1115+080 and Q 1413+117. If applicable, we replace the apparent quasar V magnitude catalog data found in Crampton et al. (1992), Jaunsen et al. (1995) and Yee et al. (1993) with more current data from Veron-Cetty & Veron (1996). We estimate the Kochanek et al. (1995) apparent quasar V magnitude data by adding the survey average V–R and V–I colours to the observational R and I magnitude data. Following K96, we only include quasars with redshift $z_\mathrm{s} > 1$. In all, our sample contains 807 singly and 5 multiply imaged quasars. The observational data of the multiply imaged quasars are summarised in Table 1. Our complete input data can be obtained from

Table 1. Observational data of multiply imaged quasars contained in the sample. The magnitudes are V magnitudes unless otherwise specified. The image separations are taken from Kochanek et al. (1997)

Identifier	m [mag]	z_s	θ [$''$]
Q 0142−100	17.0	2.72	2.2
Q 1009−0252	18.1 B	2.74	1.5
Q 1115+080	16.2	1.72	2.2
Q 1208+1011	17.9	3.80	0.48
Q 1413+117	17.0	2.55	1.2

http://multivac.jb.man.ac.uk:8000/ceres/data_from_papers/lower_limit.html

This follows K96 for purposes of comparison. Since much larger surveys (i.e. CLASS) will be considered in a future paper, there is little point in increasing the number of lenses for its own sake. Since radio observations are considered in more detail in a companion paper (Helbig et al. 1999), we restrict ourselves to optical surveys in this paper. We use the Crampton et al. (1992), HST Snapshot Survey and Yee et al. (1993) survey selection functions proposed in Kochanek (1993), the Jaunsen et al. (1995) survey selection function at $1''\!.0$ seeing and the preliminary Kochanek et al. (1995) survey selection function.

Before considering prior information in more detail, one must first decide which region of the λ_0-Ω_0 plane is to be investigated. Clearly, this region should be defined by either exact constraints or conservative estimates, as opposed to current 'best fit' values (and their errors), in order to avoid excluding any possibly viable cosmological models. Also, it is desirable for the region to be on the large side, so that in addition the sensitivity of the test (i.e. what regions of the λ_0-Ω_0 plane can be ruled out at a high confidence level) can be investigated.

3.1. The range of Ω_0 *and* λ_0

The mass clustered with galaxies on smaller scales, $\Omega_{0,\mathrm{gal}}$, is 0.1 within a factor of two (e.g. Peebles 1993). This lower limit is small compared to our full Ω_0 range so we do not assume any prior lower limit on Ω_0 except, of course,

$$\Omega_0 \geq 0. \tag{9}$$

Especially for comparison with other work it is important to note that, within the framework of cosmological models based on general relativity with which we (and almost everyone else at present) are working, $\Omega_0 \geq 0$ is a *requirement*. Results reported which include $\Omega_0 < 0$ within the errors, or even as a best-fit value, do not indicate 'implausible results' but merely improper statistics. Often, confidence contours are assumed to be ellipses and these are extended, if applicable, to $\Omega_0 < 0$. (Of course, it is possible that $\Omega_0 = 0$ is within the errors or even the best fit value for a certain set of results.)

An extremely conservative upper limit comes from dynamical tests on larger (though still cosmologically small) scales; when this work was started, we assumed an (again, extremely conservative) upper limit $\Omega_0 \leq 2$ (Czoske 1995). Since then, these methods have started to indicate smaller values of Ω_0, (e.g. da Costa et al. 1998) more in line with both a long tradition of low Ω_0 values (e.g. Gott et al. 1974; Coles & Ellis 1994, 1997) (albeit with somewhat larger errors) as well as new determinations (often with quite small errors), examples of which are mentioned in Sect. 3.2.

We have assumed no prior upper or lower limits on λ_0 per se. This has two reasons:

- 'Direct' measurements of λ_0 (as opposed to measurements of a combination of parameters involving λ_0) are virtually nonexistent.
- We obtain a small enough range in λ_0 from the values obtained from joint constraints on the range of Ω_0 and λ_0.

Historically, positive λ_0 values have been considered more than negative ones, probably because positive values can have a wide range of relatively easily observable effects, while negative ones are more difficult to measure. Many cosmological tests have a degeneracy such that λ_0 and Ω_0 are correlated, so that increasing λ_0 can be compensated for in some sense by increasing Ω_0 as well. Thus, effects of negative values of λ_0 for a given value of Ω_0 are hard to differentiate from the effects of larger values of Ω_0 for larger (less negative) values of λ_0 or even $\lambda_0 = 0$.

Here, we consider negative values of λ_0 as well. There is no a priori reason why they cannot exist. *If* one believes that the 'source' of λ_0 are zero-point fluctuations of a quantum vacuum, this would lend support to the idea that $\lambda_0 > 0$. However, it is not clear that this *must* be the *only* source of λ_0, and indeed it has been argued that, if this source of λ_0 exists, there must be an additional contribution with a *negative* value (e.g. Martel et al. 1998, though the assumption that this is possible is so obvious to the authors it is barely stated!).

In spatially closed ($k = +1$) models, the antipode is required to be at $z > 4.5$, the redshift of the most redshifted multiply imaged object currently known (Gott et al. 1989; Park & Gott 1997).[2] The light grey shaded area in Fig. 1a marks the right side of the region thus enclosed. This gives us a slightly Ω_0-dependent upper limit on λ_0 which is slightly stronger than that obtained by merely excluding models with no big bang. (This can be done because these models have a maximum redshift which is less than the redshift of high-redshift objects, the only exception being some cosmological models which have $\Omega_0 < 0.05$, the robust lower limit discussed above (e.g. Feige 1992).)

The age of the universe in units of the Hubble time, H_0^{-1}, is

$$\tau_0 = \int\limits_0^\infty \frac{\mathrm{d}z}{(1+z)\sqrt{Q(z)}}, \tag{10}$$

where $Q(z)$ is given by Eq. (2) and thus depends on Ω_0 and λ_0. (There are world models in which the maximum redshift

[2] Recently, a lensed object of even larger redshift has been detected at $z = 4.92$ (Franx et al. 1998). However, at our resolution this would make only a negligible difference to the results so we have not updated the calculations to reflect this.

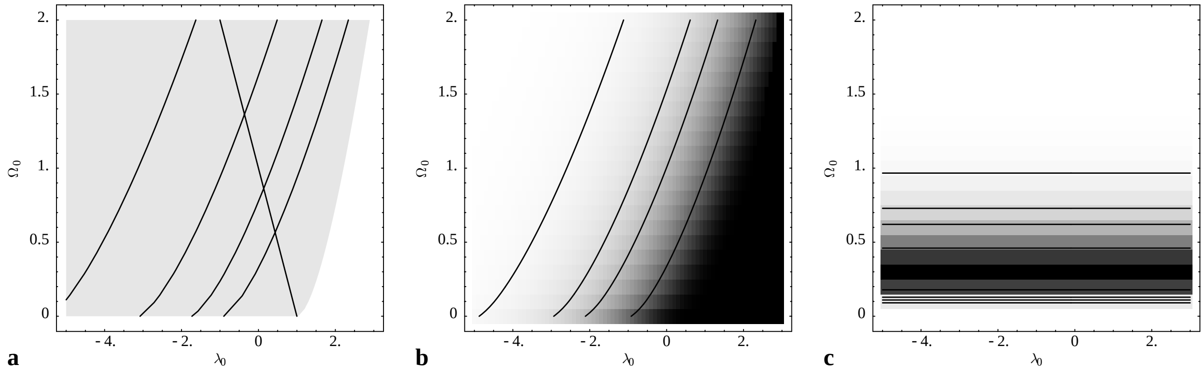

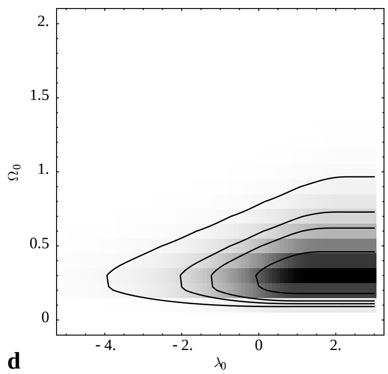

Fig. 1. a The cosmological parameter plane. The four curved lines in **a** are the isochrones $t_0 H_0 = 0.5, \ldots, 0.8$. The straight line marks spatially flat world models. In the white region, the antipodal redshift falls below $z = 4.5$, the redshift of the most redshifted multiply imaged object currently known (Gott et al. 1989; Park & Gott 1997). **b**–**d** The prior probability distributions $p_1(\lambda_0, \Omega_0)$ **b**, $p_2(\lambda_0, \Omega_0)$ **c** and $p_3(\lambda_0, \Omega_0)$ **d**. The pixel grey level is directly proportional to the probability density ratio, darker pixels reflect higher ratios. The pixel size reflects the resolution of our numerical computations. The contours mark 0.61, 0.26, 0.14 and 0.036 of the peak likelihood for the parameters λ_0 and Ω_0, which would correspond to the boundaries of the minimum 0.68, 0.90, 0.95 and 0.99 confidence regions *if the distribution were Gaussian*

is not infinite but these are all models without a big bang and are excluded by the constraint from the antipodal redshift or the lower limit on Ω_0 as discussed above and are thus not relevant for this work.) Clearly, in any physically realistic world model, $\tau_0 H_0^{-1}$ exceeds the age of the oldest galactic globular clusters:

$$\tau_0 > t_{\rm gc} H_0. \tag{11}$$

Following Carroll et al. (1992), we take a robust lower limit on λ_0 from conservative lower limits on the Hubble constant and age of the universe. This gives a lower limit on λ_0 from the value at $\Omega_0 = 0$; at larger values of Ω_0 the constraint on λ_0 is not as strict—by assuming the lower limit of $\lambda_0 = -5$ independent of Ω_0 we are being conservative. We choose $\lambda_0 \geq -5$ instead of $\lambda_0 \geq -7$ as in Carroll et al. (1992) since no published current constraints examine this region in detail. (Were this the case, then including this area would be helpful if only to aid a direct comparison.) This value corresponds roughly to the *one-sided* 99% confidence level in Fig. 1b (see Sect. 3.2), which is also a reason not to extend the area to more negative λ_0 values.

3.2. Prior probability for λ_0 and Ω_0

We have assumed no prior knowledge of λ_0 per se, apart from the upper and lower limits discussed above. This has three reasons:

- ‘Direct’ measurements of λ_0 (as opposed to measurements of a combination of parameters involving λ_0) are virtually nonexistent.
- Based on general knowledge from the literature and our own low-resolution calculations, we expect lens statistics itself to constrain λ_0 quite well.
- Although recent measurements are encouraging (see Sect. 5), the value of λ_0 is observationally not as well established as that of Ω_0.

Regarding $t_{\rm gc}$ and H_0 as independent random quantities with known prior probability density functions $p(t_{\rm gc})$ and $p(H_0)$, the probability that Eq. (11) is satisfied is

$$P(\tau_0 > t_{\rm gc} H_0) = \int_0^\infty p(H_0) \int_0^{\tau_0/H_0} p(t_{\rm gc})\, {\rm d}t_{\rm gc}\, {\rm d}H_0. \tag{12}$$

A cosmological world model is compatible with the absolute age of the oldest galactic globular clusters as long as the above expression does not vanish. Reasonably, we assume a prior probability density function that is proportional to this expression

$$p_1(\lambda_0, \Omega_0) = 1 \otimes \int_0^\infty p(H_0) \int_0^{\tau_0/H_0} p(t_{\rm gc})\, {\rm d}t_{\rm gc}\, {\rm d}H_0. \tag{13}$$

The best estimate of the absolute age of the oldest galactic globular clusters currently is $t_{\rm gc} = 11.5 \pm 1.3\,{\rm Gyr}$ (Chaboyer et al. 1998). We choose to formulate this prior information in the form of a lognormal distribution that meets these statistics

$$p(t_{\rm gc}) = L(t_{\rm gc}|11.5\,{\rm Gyr}, 1.3\,{\rm Gyr}). \tag{14}$$

Similarly, we roughly estimate $H_0 = 65 \pm 10\,{\rm km\,s^{-1}\,Mpc^{-1}}$ and choose to formulate this prior information in form of a normal distribution

$$p(H_0) = N(H_0|65\,{\rm km\,s^{-1}\,Mpc^{-1}}, 10\,{\rm km\,s^{-1}\,Mpc^{-1}}), \tag{15}$$

where the notation for L and N is such that the two arguments correspond to the mean and standard deviation.

This estimate is compatible with 'small' values of the Hubble constant, which is conservative in the sense that it restricts our region of the λ_0-Ω_0 plane less than would 'large' values. By the same token we neglect any time between the big bang and the formation of the oldest globular clusters. Inserting Eq. (14) and Eq. (15) in Eq. (13) one obtains a well-founded a priori probability distribution for the parameters Ω_0 und λ_0.

Although observational evidence has always indicated a low value of Ω_0 (e.g. Gott et al. 1974; Coles & Ellis 1994, 1997), the inflationary paradigm (e.g. Guth 1981), coupled with a prejudice against a non-negligible value of λ_0, has created a prejudice in favour of $\Omega_0 = 1$,[3] unfortunately too often to the extent where this prior belief has been elevated to the status of dogma (see, e.g., Matravers et al. 1995, for an illuminating account) even though there are serious fundamental problems with the inflationary idea (e.g. Penrose 1989) and even though there might be other solutions to the problems it claims to solve (e.g. Barrow 1995; Collins 1997). What is more, some current inflationary thinking (e.g. Turok & Hawking 1998) seems able to predict values for λ_0 and Ω_0 similar to current observationally determined values, though it would have been more interesting had this prediction been made before the recent improvements in the observational situation. (To be fair, many leading practitioners of inflation consider a flat universe to be a robust prediction and its observational falsification essentially a falsification of the entire paradigm.) Recently, in the light of overwhelming observational evidence in favour of a low value of Ω_0 (e.g. Carlberg et al. 1998b; Carlberg 1998; Carlberg et al. 1998c; Bahcall 1998; Bahcall et al. 1997; Fan et al. 1997; Bartelmann et al. 1998; Lineweaver 1998), whether determined more or less independently or in combination with other parameters, this prejudice is starting to weaken. Conservatively, these results can be summarised as

$$p_2(\lambda_0, \Omega_0) = L(\Omega_0|0.4, 0.2). \tag{16}$$

A prior constraint on Ω_0 is useful since lensing statistics alone, as expected and as our results show, cannot usefully constrain Ω_0.

In addition, we also consider the product of $p_2(\lambda_0, \Omega_0)$ with the age constraint $p_1(\lambda_0, \Omega_0)$,

$$p_3(\lambda_0, \Omega_0) = p_1(\lambda_0, \Omega_0) \otimes p_2(\lambda_0, \Omega_0). \tag{17}$$

3.3. General discussion of prior information

Using harsher constraints would mean that results would reflect almost exclusively the prior information as opposed to the information derived from lensing statistics. It is not the purpose of this paper to do a joint analysis of several cosmological tests,[4] but rather to examine lens statistics as a cosmological test. For practical reasons, an upper limit on Ω_0 and upper and lower limits on λ_0 are required. On the other hand, it is sensible to combine the results with conservative constraints from other well-understood cosmological tests where there is general agreement and little room for debate. Within our upper and lower limits, we present our results both with and without the constraints discussed above. The density values and confidence contours of the three prior probability density functions are shown in Fig. 1b–d.

[3] After this was found to conflict with too many observations, the prejudice against a non-negligible value of λ_0 weakened, and the new prejudice has been in favour of a flat universe with $\lambda_0 + \Omega_0 = 1$.

[4] but see Sect. 5

4. Calculations

Following K96, we use the Hinshaw & Krauss (1987) softened isothermal sphere model for modeling the light deflection properties of the lens galaxies. For this model, the lens equation reads

$$x - y = \frac{bx}{\hat{s} + \sqrt{x^2 + \hat{s}^2}}, \tag{18}$$

where x is the angular position in the lens plane, y the angular position in the source plane, $b \equiv 4\pi(\sigma/c)^2(D_{\rm ds}/D_{\rm os})$, σ denotes the one–dimensional velocity dispersion of the dark matter, s denotes the core radius, $\hat{s} \equiv s/D_{\rm od}$ is the angular core radius and $D_{\rm od}$, $D_{\rm os}$ and $D_{\rm ds}$ denote the angular size distances between the observer and the lens galaxy, the observer and the source and the lens galaxy and the source, respectively. Still following K96, we model the distribution of elliptical and lenticular lens galaxies using Schechter functions with constant comoving density

$$n_{\rm e} = 0.61 \pm 0.21\, h^3\, 10^{-2}\,\text{Mpc}^{-3} \tag{19}$$

($h = H_0\, 10^{-2}\,\text{km}^{-1}\,\text{s Mpc}$) and slope

$$\alpha_{\rm e} = -1.0 \pm 0.15. \tag{20}$$

The lens galaxy luminosities are converted to the dark matter velocity dispersions of the softened isothermal lens model by means of Faber–Jackson type relations,

$$L/L_{*\rm e} = (\sigma/\sigma_{*\rm e})^{\gamma_{\rm e}}, \tag{21}$$

where

$$\gamma_{\rm e} = 4.0 \pm 0.5 \tag{22}$$

and

$$\sigma_{*\rm e} = 225.0 \pm 22.5\,\text{km}\,\text{s}^{-1}. \tag{23}$$

The core radii of the softened isothermal lens model are varied with the dark matter velocity dispersions according to

$$s/s_{*\rm e} = (\sigma/\sigma_{*\rm e})^{2+\varepsilon}, \tag{24}$$

where $\varepsilon = 2.8$ and $s_{*\rm e} = 10h^{-1}$ pc. We consider elliptical and lenticular lens galaxies only. For the number–magnitude counts of quasars, we adopt the best-fit model from K96. We neglect here evolution, dust and other possible systematic effects and refer the reader to K96 for a discussion.

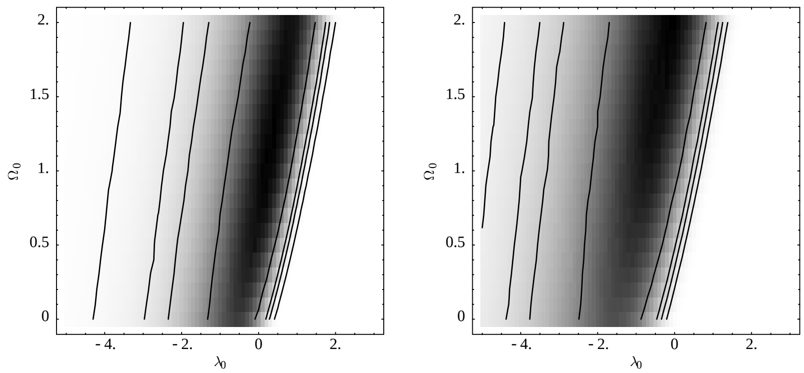

Fig. 2. *Left panel:* The likelihood function $p(D|\lambda_0, \Omega_0, \boldsymbol{\xi}_0)$. All nuisance parameters are assumed to take precisely their mean values. The pixel grey level is directly proportional to the likelihood ratio, darker pixels reflect higher ratios. The pixel size reflects the resolution of our numerical computations. The contours mark the boundaries of the minimum 0.68, 0.90, 0.95 and 0.99 confidence regions for the parameters λ_0 and Ω_0. *Right panel:* Exactly the same as the left panel, but the parameter $n_{\rm e}$ is increased by two standard deviations

In our first calculations we apply Eq. (8) and compute the a priori likelihood

$$p(D|\lambda_0, \Omega_0, \boldsymbol{\xi}_0) \tag{25}$$

and the posterior probability density functions

$$p_1(\lambda_0, \Omega_0|D) = p(D|\lambda_0, \Omega_0, \boldsymbol{\xi}_0) \otimes p_1(\lambda_0, \Omega_0), \tag{26}$$

$$p_2(\lambda_0, \Omega_0|D) = p(D|\lambda_0, \Omega_0, \boldsymbol{\xi}_0) \otimes p_2(\lambda_0, \Omega_0), \tag{27}$$

and

$$p_3(\lambda_0, \Omega_0|D) = p(D|\lambda_0, \Omega_0, \boldsymbol{\xi}_0) \otimes p_3(\lambda_0, \Omega_0) \tag{28}$$

in the limit where all nuisance parameters take precisely their mean values. To obtain an impression of the consequences of neglecting the uncerntainties of the nuisance parameters, in our second calculation we increase the value of the most uncertain nuisance parameter, $n_{\rm e}$, by two standard deviations.

For the computation of the innermost integral on the right side of Eq. (3), we consider the detectability of images in pairs: If the separation between the two closest images – these are always images 2 and 3, counting from the outside in – is more than the lower limit of the survey resolution limit $S(y)$, we define the image separation and flux ratio for the purpose of sample selection based on the two brightest images, usually 1 and 2. Otherwise we construct one image from the combined fluxes and flux-weighted positions of images 2 and 3 and define the image separation and flux ratio for the purpose of sample selection based on this combination image and image 1.

In general, if the separation between images 1 and 2 is too large for the survey *and* the separation between images 2 and 3 is large enough, then the image separation and flux ratio for the purpose of sample selection should be based on images 2 and 3. However, the present surveys are sensitive to the largest separations due to isolated galaxies, so this case doesn't need to be addressed in this paper (i.e. implementing it would lead to the same results in the present case).

For the calculation of the probabilities $p(m_i, z_i, \theta_i)$ the function $C(y)$ selects only those image configurations whose separation is ± 10 per cent of the observed separation θ_i.

Each of the three integrals on the right side of Eq. (3) is approximated to an accuracy better than 0.004 by a family of recursive monotone stable formulae (Favati et al. 1991a,b).

5. Results and discussion

5.1. Information content

Given some observational data D, some model parameters $\boldsymbol{\phi}$, and some prior and posterior probability density functions $p(\boldsymbol{\phi})$ and $p(\boldsymbol{\phi}|D)$, the amount of information obtained from the data (e.g. Bernardo & Smith 1994) (on a logarithmic scale) is

$$\log[I(D)] = \int p(\boldsymbol{\phi}) \log\left[\frac{p(\boldsymbol{\phi}|D)}{p(\boldsymbol{\phi})}\right] \mathrm{d}\boldsymbol{\phi}. \tag{29}$$

The amounts of information obtained from our sample data are given in the caption of Fig. 3.

5.2. Results

The left panel of Fig. 2 shows the constraints on the cosmological parameters λ_0 and Ω_0 based only on the information obtained from the lens statistics.

Quite good constraints can be placed on λ_0, more or less independent of Ω_0. It is a well-known fact (see K96 and references therein) that lensing statistics can provide a good *upper* limit on λ_0. While in the past this has mainly been discussed in the context of flat cosmological models, it is of course more general (Carroll et al. 1992; Falco et al. 1998). Although no unexpected effects are seen, it is important to note that this is the first time λ_0 and Ω_0 have been used as independent parameters in conjunction with a non-singular lens model in an analysis of this type.

Our analysis shows for the first time that gravitational lensing statistics can place a quite firm *lower* limit on λ_0 as well, again more or less independent of Ω_0. The constraint is not as tight since the gradient in the probability density is not as steep towards negative λ_0 as towards positive λ_0. If this lower limit can be improved enough, it could provide an independent confirmation of the detection of a positive cosmological constant (see Sect. 5.3). On the other hand, this might be difficult, since Poisson errors in the number of lenses and uncertainties in the normalisation of the luminosity density of galaxies introduce relatively large uncertainties in this region of parameter space (K96, Falco et al. 1998). The latter effect is illustrated in the right panel of Fig. 2, where $n_{\rm e}$, the galaxy luminosity density normalisation, is increased by two standard deviations: the derived lower limit on λ_0 changes much more than does the upper

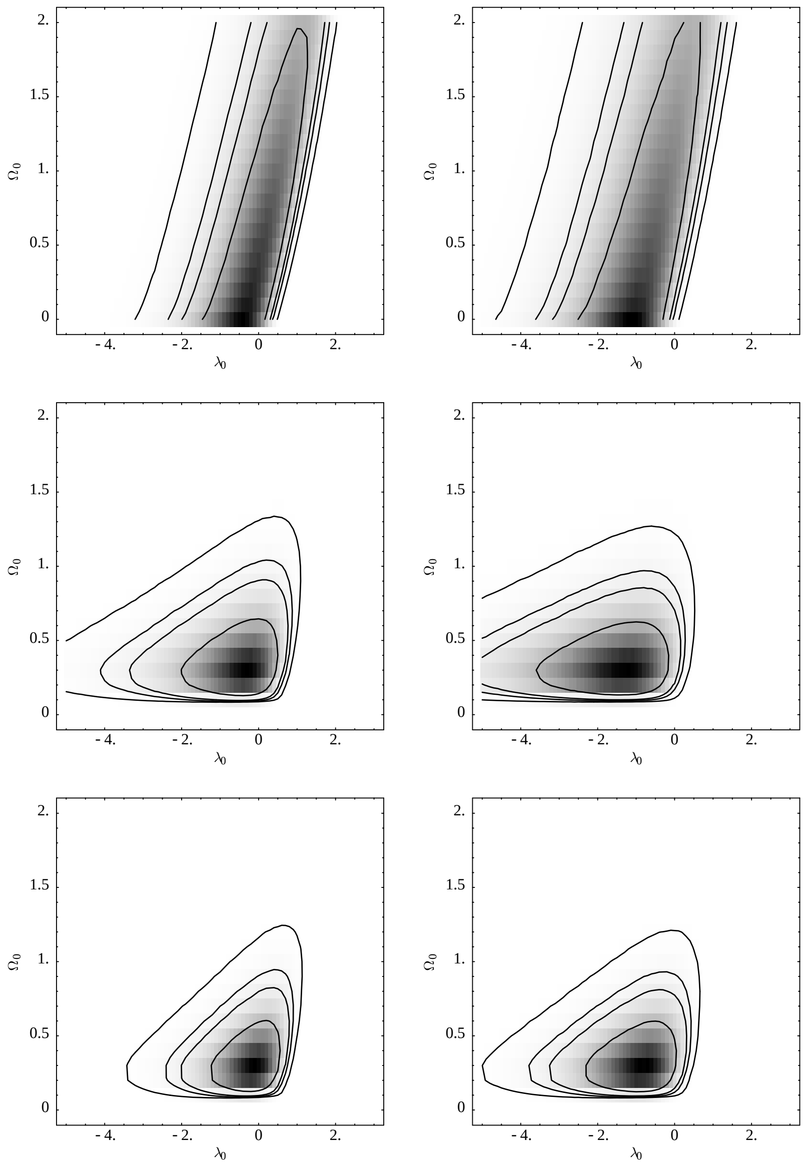

Fig. 3. *Left column:* The posterior probability density functions $p_1(\lambda_0, \Omega_0|D)$ (top panel), $p_2(\lambda_0, \Omega_0|D)$ (middle panel) and $p_3(\lambda_0, \Omega_0|D)$ (bottom panel). All nuisance parameters are assumed to take precisely their mean values. The pixel grey level is directly proportional to the likelihood ratio, darker pixels reflect higher ratios. The pixel size reflects the resolution of our numerical computations. The contours mark the boundaries of the minimum 0.68, 0.90, 0.95 and 0.99 confidence regions for the parameters λ_0 and Ω_0. The respective amounts of information (Eq. (29)) obtained from our sample data are $I_1 = 1.74$, $I_2 = 1.24$ and $I_3 = 1.74$. *Right column:* Exactly the same as the left column, but the parameter $n_{\rm e}$ is increased by two standard deviations

limit. Nevertheless, our robust lower limit is much better than the -7 mentioned in Carroll et al. (1992).

Our results place no useful constraints on Ω_0. It is interesting to note the fact, however, that likely values of λ_0 and Ω_0 are positively correlated. This is similar to most cosmological tests, a notable exception being constraints derived from CMB anisotropies (see Sect. 5.3). Fortunately, constraints on Ω_0 from other sources are quite good (Sect. 3.2). Often, this is cast in the form of a constraint on $\Omega_0 - \lambda_0$ (e.g. Cooray et al. 1999) or, perhaps more practical, $\lambda_0 - \Omega_0$. This is a reasonable way or reducing the information to one number, at least when one is concerned with upper limits on λ_0 (or $\lambda_0 - \Omega_0$) in a relatively low-density universe. Besides the obvious dependencies on confidence levels and assumptions made, when comparing constraints on λ_0 from different investigations one should keep in mind whether they are approximations, like $\lambda_0 - \Omega_0$ in lensing statistics, and whether a value for a particular scenario (for example, for a flat universe) is the 'obvious' definition or in fact describes the intersection of the $k = 0$ line with the corresponding 2-dimensional confidence contour, which in general will give a different number. Also, some authors plot 'real' confidence contours while some actually plot contours at values which would correspond to certain confidence contours were the likelihood distribution in the parameter space in question Gaussian.

The left plot in the top row of Fig. 3 shows the joint likelihood of our lensing statistics analysis and that obtained by using conservative estimates for H_0 and the age of the universe (see Sect. 3.2). Although neither method alone sets useful constraints on Ω_0, their combination does, since the constraint involving H_0 and the age of the universe only allows large values of Ω_0 for λ_0 values which are excluded by lens statistics. Even though the 68% contour still allows almost the entire Ω_0 range, it is obvious from the grey scale that much lower values of Ω_0 are

Table 2. Marginal mean values, standard deviations and 0.95 confidence intervals for the parameter λ_0 on the basis of the marginal distributions shown in the top row of Fig. 4; 'information' refers to Eq. 29

Distribution	Mean	standard deviation	95% c.l. range		information
$p(D\|\lambda_0)$	-0.35	1.07	-2.55	1.51	
$p_1(\lambda_0\|D)$	-0.02	0.80	-1.59	1.50	1.74
$p_2(\lambda_0\|D)$	-0.78	0.97	-2.85	0.76	1.24
$p_3(\lambda_0\|D)$	-0.34	0.67	-1.72	0.79	1.74

favoured by the joint constraints. The upper limit on λ_0 changes only slightly while, as is to be expected, the lower limit becomes tighter. Also, the change caused by increasing $n_{\rm e}$ by 2 standard deviations is less pronounced, with regard to both lower and upper limits on λ_0, as demonstrated in the right plot in top row of Fig. 3.

The middle row of Fig. 3 shows the effect of including our prior information on Ω_0 (see Sect. 3.2). As is to be expected, (for both values of $n_{\rm e}$) lower values of Ω_0 are favoured. This has the side effect of weakening our lower limit on λ_0 (though only slightly affecting the upper limit).

We believe that the left plot of the bottom row of Fig. 3 represents very robust constraints in the λ_0-Ω_0 plane. The upper limits on λ_0 come from gravitational lensing statistics, which, due to the extremely rapid increase in the optical depth for larger values of λ_0, are quite robust and relatively insensitive to uncertainties in the input data (compare the left and right columns of Fig. 3) as well as to the prior information used data (compare the upper, lower and middle rows of Fig. 3). The upper and lower limits on Ω_0 are based on a number of different methods and appear to be quite robust, as discussed in Sect. 3.2. The combination of the relatively secure knowledge of H_0 and the age of the universe combine with lens statistics to produce a good lower limit on λ_0, although this is to some extent still subject to the caveats mentioned above.

If one is interested in the allowed range of λ_0, one can marginalise over Ω_0 to obtain a probability distribution for λ_0. This is illustrated in Fig. 4 and Table 2.

5.3. Comparison with other results

For comparison with other results, as a first step one can examine the allowed range of λ_0 for the current 'best-fit' value for Ω_0, which we take, based on the work cited in Sect. 3.2, to be $\Omega_0 = 0.3$. (A more conservative estimate is reflected by using the prior probability distribution $p_2(\lambda_0, \Omega_0) = L(\Omega_0|0.4, 0.2)$ as shown by the dark grey curve in Fig. 4 and in Table 2.) On the other hand, previous limits on λ_0 have often been quoted for a flat universe (K96 and references therein). We consider both cases in Tables 3 and 4.

We do not do a comparison for the special case $\lambda_0 = 0$ since this analysis of gravitational lensing statistics does not usefully constrain Ω_0 (any limits coming only from the prior information on Ω_0).

It is beyond the scope of this paper to do a full comparison of different cosmological tests. Except for a few general comments, we therefore restrict ourselves to comments on the similarities and differences between the results from this work without using prior information on λ_0 and Ω_0, i.e. (the left plot in) Fig. 2, and the those from K96 and Falco et al. (1998) (using only optical data, i.e. the lower left plot in their Fig. 5).

Taking all results at face value and examining the $\Omega_0 = 0.3$ case first, we note that with 'three-and-one-half' exceptions (counting as one test each the four from this work and the three from Falco et al. (1998)) the 68% c.l. *lower* limit from Lineweaver (1998) is *higher* than *all* 68% *upper* limits from other tests, while the 95% lower and upper confidence levels from Lineweaver (1998) are higher than the corresponding limits from the other tests for all but one of these. Even at the 99.9% confidence level (not shown in Table 3), the Lineweaver (1998) result requires $\lambda_0 \geq 0.12$. If one assumes $\Omega_0 = 0.3$, only Lineweaver (1998) requires $\lambda_0 > 0$, though all other tests (except Carlberg (1998)) are compatible with this. This is not surprising, since it is well-known that constraints from CMB anisotropies tend to run more or less orthogonal in the λ_0-Ω_0 plane to those from most other tests (e.g. White 1998; Eisenstein et al. 1998b; Tegmark et al. 1998a,b).

Examining the $k = 0$ case, it is interesting to note that the 68% (90%) confidence level *lower* limit on λ_0 from Carlberg (1998) is *higher* than *all* of the 68% (90%) c.l. *upper* limits from *all* other tests except Guerra et al. (1998). Otherwise, with 'one-and-one-half' exceptions all tests are compatible even at the 68% confidence level. If one assumes $k = 0$, then the evidence for $\lambda_0 > 0$ looks convincing: at the 68% confidence level, again with 'one-and-one-half' exceptions, all tests indicate $\lambda_0 > 0$; even at 90% the evidence is still quite good, if one keeps in mind that the gradient towards smaller values of λ_0 is generally not as steep as towards larger values.

Again taken at face value, neither the $k = 0$ case nor the $\Omega_0 = 0.3$ case are compatible with all tests, even at the ≈90% confidence level. It appears the simplest solution to achieve concordance would be to have $\Omega_0 \approx 0.2$, which is within the error on Ω_0 discussed in Sect. 3.2. For $k = 0$ this would imply $\lambda_0 = 0.8$, which seems to be ruled out, thus ruling out the flat universe altogether. For a non-flat universe, reducing Ω_0 would, due to the CMB constraint, require a higher value of λ_0, and thus make the $\lambda_0 = 0$ case more unlikely, ruling out this special case as well.

On balance, a cosmological model with $\lambda_0 \approx 0.3$ and $\Omega_0 \approx 0.25$ seems compatible with all known observational data (not just those discussed here) at a comfortable confidence level.

For a 'likely' Ω_0 value of 0.3 we have calculated the likelihood with the higher resolution $\Delta\lambda_0 = 0.01$. This is shown in Fig. 5. From these calculations one can extract confidence limits which, due to the higher resolution in λ_0, are more accurate. These are presented in Table 5 and should be compared to those for $p(D|\lambda_0)$ from Table 3.

Again, a full discussion of joint constraints involving discussion of possible sources of error for each test, as well as comparing the full contours in the λ_0-Ω_0 plane, is beyond the

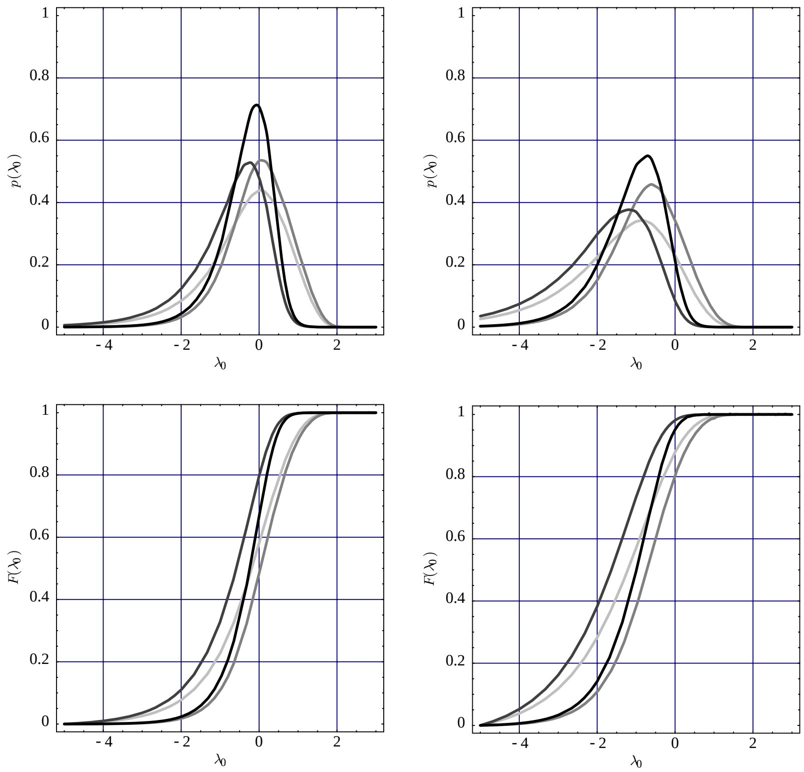

Fig. 4. *Left column:* The top panel shows the normalised marginal likelihood function $p(\lambda_0|D)$ (light grey curve) and the marginal posterior probability density functions $p_1(D|\lambda_0)$ (medium grey curve), $p_2(D|\lambda_0)$ (dark grey curve) and $p_3(D|\lambda_0)$ (black curve). All nuisance parameters are assumed to take precisely their mean values. The bottom panel shows the respective cumulative distribution functions. These can be used to construct any desired Ω_0-averaged upper or lower limits on λ_0. *Right column:* Exactly the same as the left column, but the parameter $n_{\rm e}$ is increased by two standard deviations

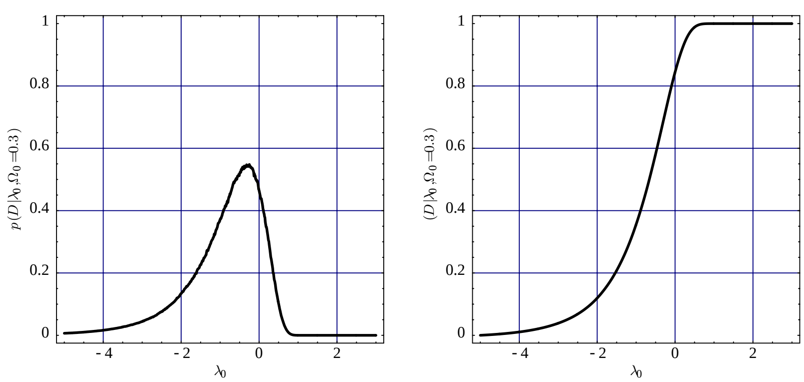

Fig. 5. *Left panel:* The likelihood function as a function of λ_0 for $\Omega_0 = 0.3$ and with all nuisance parameters taking their default values. *Right panel:* The same but plotted cumulatively. See Table 5

scope of this paper. However, quick comparisons would be aided were the results of all tests available in an easy-to-process electronic form (see below); such quick consistency tests would enable one to spot areas of inconsistency much more quickly. Also, it should be emphasised that the projections onto the λ_0-axis of the intersection of a particular confidence contour with the $\Omega_0 = 0.3$ or $k = 0$ axis are generally *not* the same as the corresponding confidence interval for the $\Omega_0 = 0.3$ or $k = 0$ special cases.

For a flat universe, our 95% confidence level upper limit on λ_0-Ω_0, i.e. the value of λ_0 where this contour crosses the $k = 0$ line, is $\lambda_0 < 0.62$. This is essentially the same as the $\lambda_0 < 0.66$ of K96, as was to be expected considering we used essentially the same data and methods. Interpreted cautiously, one might conclude from this that the singular isothermal sphere model is a good approximation as far as determining the cosmological parameters from lens statistics is concerned, as was assumed in Falco et al. (1998). Our 99% confidence level upper limit on λ_0 is $\lambda_0 < 0.70$. This is quite a tight upper bound on λ_0 and appears to be quite robust.

Perhaps more interesting is the comparison with (the results using only optical data in) Falco et al. (1998). Although a detailed comparison is complicated by the different plotting scheme and reducing the entire contour (or indeed grey-scale) plot to a few numbers throws away information, it is obvious that the plots are broadly similar. Our 68% contour is, for $\Omega_0 \approx 1$, roughly parallel to the λ_0-axis at $\lambda_0 \approx -1$. This is just at the edge of the Falco et al. (1998) plot, and as they provide no grey-scale, it is difficult to compare the lower limits on λ_0. Thus, while our main goal was to explore a 'large enough' region of parameter space, comparison in the areas where there is overlap shows consistency, which strengthens our faith in the conclusions pertaining to areas of parameter space where there is no overlap.

Recently, it has become quite fashionable to discuss joint constraints derived from a variety of cosmological tests. This

Table 3. Mean values and ranges for assorted confidence levels for the parameter λ_0 for our a priori and various a posteriori likelihoods from this analysis and from other tests from the literature (using the latest publicly available results) for the special case $\Omega_0 = 0.3$. Except where noted, the ranges quoted are the projections of the corresponding confidence contours in the λ_0-Ω_0 plane onto the λ_0 axis[a] (as opposed to Ω_0-independent estimates, which of course would always give a smaller range), and are of course two-sided, not one-sided, bounds. Values are either those quoted in the references given and/or obtained from figures in those references; inequalities mean that the corresponding confidence contour is to be found in the range indicated by the inequality, e.g. < -1.2 would mean that the corresponding contour level is to be found at $\lambda_0 < -1.2$, *not* that the constraint is $\lambda_0 < -1.2$ at the corresponding confidence level. This arises because the corresponding area of parameter space was not examined in the reference in question. If the confidence interval could not be determined from the reference, *both* values in the corresponding column are missing

Cosmological test	68% c.l. range		90% c.l. range		95% c.l. range		99% c.l. range	
this work, $p(D\|\lambda_0)$	-1.18	0.24	-2.19	0.50	-2.81	0.60	-4.16	0.73
this work, $p_1(\lambda_0\|D)$	-0.97	0.46	-1.55	0.60	-1.89	0.69	-2.73	0.81
this work, $p_2(\lambda_0\|D)$	-2.00	0.49	-3.33	0.65	-4.10	0.72	< -5.00	0.80
this work, $p_3(\lambda_0\|D)$	-1.20	0.52	-1.98	0.69	-2.35	0.77	-3.40	0.86
lens statistics (K96)	not possible since only $k = 0$ models considered							
radio lenses[bc]	-0.54	0.28	< -1.00	0.75	< -1.00	0.89		
optical lenses[de]	< -1.00	0.37	< -1.00	0.75	< -1.00	0.89		
radio + optical lenses[fg]	< -1.00	-0.12	< -1.00	0.50	< -1.00	0.70	< -1.00	0.89
supernovae m-z relation $\mathcal{A}$[h]	-0.70	0.50	-1.15	0.75				
supernovae m-z relation $\mathcal{B}$[ijk]	0.78	1.00			0.53	1.27	0.27	1.41
CNOC survey[l]	< -0.50	< -0.50	< -0.50	< -0.50				
CMB[mn]	0.44	0.67			0.36	> 0.90	0.26	> 0.90
CMB + *IRAS*[o]	not possible since only $k = 0$ models considered							
double radio sources[p]	0.00	1.00	< -2.00	1.39				

[a] Note that some references quote confidence ranges for $k = 0$—in general, these will be different than the projection of the intersection of the corresponding contour in the λ_0-Ω_0 plane onto the λ_0-axis.
[b] Falco et al. (1998)
[c] contour at 95.4% not 95%
[d] Falco et al. (1998)
[e] contour at 95.4% not 95%
[f] Falco et al. (1998)
[g] contour at 95.4% not 95%
[h] Perlmutter et al. (1998)
[i] Riess et al. (1998)
[j] Fig. 6, solid contours
[k] contours at 68.3%, 95.4% and 99.7% instead of 68%, 95% and 99% respectively
[l] Carlberg (1998)
[m] Lineweaver (1998)
[n] contours at 68.3%, 95.4% and 99.7% instead of 68%, 95% and 99%, respectively
[o] Webster et al. (1998)
[p] Guerra et al. (1998)

has grown from plotting the overlap of likelihood contours (often in a space spanned by parameters other than λ_0 and Ω_0) (e.g. Ostriker & Steinhardt 1995; Turner 1996; Bagla et al. 1996; Krauss 1998; White 1998) to full-blown joint likelihood analyses, both detailed theoretical investigations of what will be possible in the future (e.g. Tegmark et al. 1998a,b; Eisenstein et al. 1998a,b) and more restricted analyses using present data (e.g. Webster et al. 1998). While in some cases it is quick and easy to calculate the likelihood as a function of λ_0 and Ω_0 given the data, for example for tests using the m-z relation, in other cases such as the present one it is a major programming and computational effort to do so. To aid comparisons, all figures from this paper are available in the form of tables of numbers at

```
http://multivac.jb.man.ac.uk:8000/ceres
/data_from_papers/lower_limit.html
```

and we urge our colleagues to follow our example. We applaud the fact that most results are now presented in the λ_0-Ω_0 plane, as opposed to using other parameters such as q_0 or $\Omega_{\rm tot} \equiv \lambda_0 + \Omega_0$. A further aid in comparison would be a uniform choice of axes. We prefer to plot Ω_0 on the y-axis and λ_0 on the x axis since up/down symmetry is less fundamental than left/right symmetry and this mirrors the fact that Ω_0 has the physical lower limit $\Omega_0 = 0$ whereas no corresponding upper or lower limits for λ_0 exist. Square plots with the same range would further aid the comparison. Of course, if all data are publicly available, then they can be re-plotted to taste.

Table 4. Mean values and ranges for assorted confidence levels for the parameter λ_0 for our a priori and various a posteriori likelihoods from this analysis and from other tests from the literature (using the latest publicly available results) for the special case $k = 0$. Otherwise the same as Table 3, in particular the references are not listed in the footnotes to this table. X denotes the fact that there is no intersection of the confidence contour with the $k = 0$ line

Cosmological test	68% c.l. range		90% c.l. range		95% c.l. range		99% c.l. range	
this work, $p(D\|\lambda_0)$	-0.68	0.51	< -1.00	0.57	< -1.00	0.62	< -1.00	0.70
this work, $p_1(\lambda_0\|D)$	-0.09	0.56	-0.38	0.64	-0.57	0.68	-1.04	0.81
this work, $p_2(\lambda_0\|D)$	X	X	0.09	0.69	-0.03	0.73	-0.28	0.92
this work, $p_3(\lambda_0\|D)$	0.47	0.48	0.18	0.67	0.07	0.70	-0.14	0.84
lens statistics[a]					< 0.00	0.66		
radio lenses[b]	-0.47	0.56	< -1.00	0.72	< -1.00	0.80	< -1.00	0.85
optical lenses[c]	< -1.00	0.56	< -1.00	0.72	< -1.00	0.80	< -1.00	0.87
radio + optical lenses[d]	-0.87	0.43	< -1.00	0.60	< -1.00	0.69	< -1.00	0.78
supernovae m-z relation $\mathcal{A}$	0.20	0.60	-0.05	0.75				
supernovae m-z relation $\mathcal{B}$[ef]	0.74	0.83			0.61	0.92	0.50	1.00
CNOC survey	0.85	0.95	0.81	0.98				
CMB[g]	< 0.00	0.60	< 0.00	< 0.00	< 0.00	< 0.00	< 0.00	< 0.00
CMB + *IRAS*[h]	0.47	0.71						
double radio sources	0.35	1.00	0.70	1.00				

[a] value for $k = 0$, not projection
[b] contour at 95.4% not 95%
[c] contour at 95.4% not 95%
[d] contour at 95.4% not 95%
[e] Fig. 6, solid contours
[f] contours at 68.3%, 95.4% and 99.7% instead of 68%, 95% and 99% respectively
[g] contour at 68.3% instead of 68%; other contours, and part of the 68.3% contour, lie partially in the $k = +1$ area of parameter space which was not examined for technical reasons in Lineweaver (1998)
[h] value for $k = 0$, not projection

Table 5. Confidence ranges for λ_0 assuming $\Omega_0 = 0.3$. Unlike the results presented in Table 3, these figures are for a specific value of Ω_0 and not the values of intersection of particular contours with the $\Omega_0 = 0.3$ line in the λ_0-Ω_0 plane. These are more appropriate if one is convinced that $\Omega_0 = 0.3$ and have been calculated using ten times better resolution than the rest of our results presented in this work. See Fig. 5

68% c.l. range		90% c.l. range		95% c.l. range		99% c.l. range	
-1.27	0.27	-2.26	0.51	-2.87	0.60	-4.10	0.72

6. Summary and conclusions

We have re-analysed optical gravitational lens surveys from the literature, using the techniques described in Kochanek (1996), for the first time allowing both the cosmological constant λ_0 and the density parameter Ω_0 to be free parameters while also using a non-singular lens model. We confirm the well-known results that gravitational lensing statistics can provide a good upper limit on λ_0 but are relatively insensitive to Ω_0. We have presented the new result of a robust lower limit on λ_0, which is a substantial improvement on previously known *robust* lower limits. Coupled with relatively conservative prior information about the Hubble constant H_0, the age of the universe and the well-established value of Ω_0, one can reduce the allowed parameter space in the λ_0-Ω_0 plane to a small, finite region, which is similar to the area allowed by joint constraints based on many other cosmological tests (see Fig. 3).

Using lens statistics information alone, at 95% confidence, our lower and upper limits on $\lambda_0 - \Omega_0$ are respectively -3.17 and 0.3. For a flat universe, this corresponds to lower and upper limits on λ_0 of respectively -1.09 and 0.65. Keeping in mind the difficulties of a quantitative comparison, this is in good agreement with other recent measurements of the cosmological constant. This value was calculated from Table 5 and assuming a degeneracy in $\lambda_0 - \Omega_0$ as in Cooray et al. (1999) and Cooray (1999). For comparison, from Table 4, the corresponding value for the upper limit on λ_0 is 0.62 and the value from K96 is 0.66.[5]

For detailed comparison of cosmological tests, one needs to compare confidence contours—calculated in the same, preferably in the 'real', way—in the same parameter space. Of course, this makes it difficult to meaningfully reduce the results of a given cosmological test to one or even a few single numbers. Unless a cosmological test is developed which can measure λ_0 independently of any other parameters, there is not much point in quoting unqualified 'limits on λ_0'.

[5] The value from Cooray et al. (1999) and Cooray (1999) is 0.79, but it should be noted this value (the same in both papers) is based on different surveys, namely the Hubble Deep Field and CLASS, respecively.)

Presently tentative claims of the detection of a positive cosmological constant, if true, would rank among the great discoveries of cosmology. Even though there are serious difficulties involved, it seems worthwhile to be able to confirm this result by improving the lower limit on λ_0 derived from gravitational lensing statistics. Targetting the two primary sources of uncertainty calls for improving our knowledge of the normalisation of the local luminosity density of galaxies as well as increasing the size of gravitational lens surveys. As far as the latter goes, the CLASS survey (Browne et al. 1998; Myers et al. 1999) looks the most promising at the moment. In a companion paper (Helbig et al. 1999), we have shown that comparable constraints to the ones presented in this work can be obtained from the JVAS gravitational lens survey; this gives us hope that the much larger CLASS survey will offer improvement in this area.

Cosmological tests which set tight upper limits on Ω_0 imply, for a flat $k = 0$ universe, a value of λ_0 which is ruled out by lensing statistics. For a non-flat universe, many tests are indicating $\lambda_0 > 0$, and at present a cosmological model with $\lambda_0 \approx 0.3$ and $\Omega_0 \approx 0.25$ seems compatible with all known observational data, with neither a flat universe nor a universe without a positive cosmological constant being viable alternatives. The simplest case, the Einstein-de Sitter universe with $\lambda_0 = 0$ and $\Omega_0 = 1$, both flat and without a cosmological constant, had been abandoned long before the new observational data cited in this work came to light (see, e.g., Ostriker & Steinhardt 1995, and references therein); this trend has continued, with the next-most-simple cases also no longer viable. For λ_0 and Ω_0, we have in a sense reached the least simple case; it will be interesting to see if this trend continues with regard to the other cosmological parameters, in particular those which can be measured by the *Planck Surveyor* mission. Larger gravitational lens surveys such as CLASS will be a step in this direction.

Acknowledgements. We thank Sjur Refsdal, Leon Koopmans, Lutz Wisotzki and many colleagues at Jodrell Bank for helpful comments and suggestions. This research was supported in part by the European Commission, TMR Programme, Research Network Contract ERBFMRXCT96-0034 'CERES'.

Appendix A: getting a feel for it

The likelihood of a given cosmological model for a given set of observational data, calculated using Eq. (3), is the result of the complex interplay of many factors. While this is necessary for a detailed analysis, it perhaps obscures the fact that the likelihood is basically the product of two terms, the likelihood that the non-lenses in our sample are not lenses (see Fig. A1) and the likelihood that the lenses in our sample (see Fig. A2) have the observed properties.[6] The latter in turn is the result of two basic effects: the dependency of the volume element $\mathrm{d}V/\mathrm{d}z$ on λ_0 and Ω_0 (see Fig. A3) and the dependency on the lensing cross section on λ_0 and Ω_0 (see Fig. A4). One can also use the probability that the non-lenses in our sample are not lenses (illustrated in Fig. A1) to calculate the expected number of lenses in our sample (see Fig. A5), although obviously just counting the number of lenses does not make use of as much of the available information as does using Eq. (3).

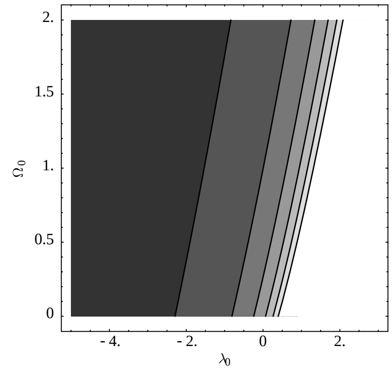

Fig. A1. Likelihood that the non-lenses in our sample are not lenses. The contour levels mark changes of a factor of ten in the probability, which is also indicated by the grey scale, darker values corresponding to higher values

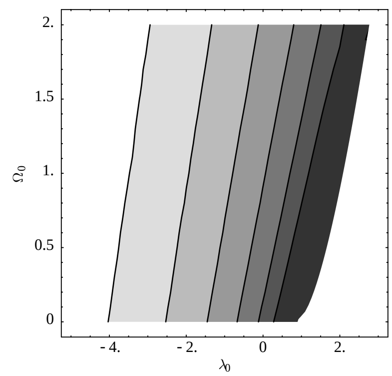

Fig. A2. Likelihood that the lenses in our sample have the properties they do. The contour levels mark changes of a factor of ten in the probability, which is also indicated by the grey scale, darker values corresponding to higher values

[6] It is interesting to note that the measurement of λ_0 by Im et al. (1997) (who obtain $\lambda_0 = 0.64^{+0.15}_{-0.26}$ for a flat universe and thus a lower limit) essentially corresponds to Fig. A2 (though with a different sample of lenses). Since lensing is a rare phenomenon, small-number statistics are a source of concern. The advantage of a well-defined *gravitational lens survey*, as opposed to using a 'sample from the literature', is that the (much greater) number of non-lenses in the sample also makes a contribution. A comparison of Figs. A1 and A2 hints that not taking the non-lenses into account would tend to favour a high value of λ_0, as indeed found by Im et al. (1997).

References

Bagla J.S., Padmanabhan T., Narlikar J.V., 1996, Comments Astrophys. 18, 275
Bahcall N., Fan X., Cen R., 1997, ApJ 485, L53

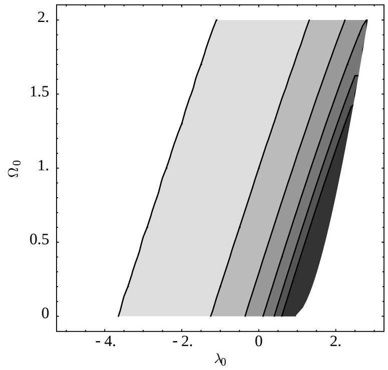

Fig. A3. The volume element $\mathrm{d}V/\mathrm{d}z$ at the typical lens galaxy redshift $z_\mathrm{d} = 0.7$. The contours indicate the fraction $0.1, 0.2, \ldots 0.6$ of the volume element in the limiting case of the de Sitter model ($\lambda_0 = 1$, $\Omega_0 = 0$). This is also indicated by the grey scale, darker values corresponding to a larger volume. For smaller redshifts the contours are more vertical (and further apart), for larger redshifts more horizontal (cf. Fig. 3 of Tegmark et al. (1998b) but note their swapped axes)

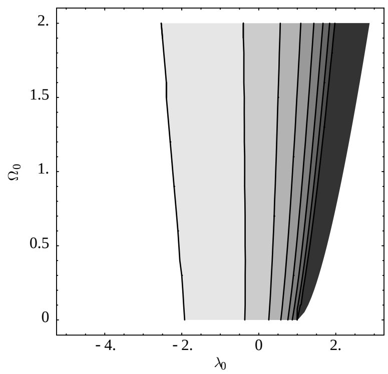

Fig. A4. Cross section for the softened singular isothermal sphere model used in this work for a typical lens redshift $z_\mathrm{d} = 0.7$ and a typical source redshift $z_\mathrm{s} = 2.0$ for the fiducial values $\sigma = \sigma_*$ and $s = s*$ (see Sect. 4). The contours indicate the fraction $0.3, 0.4, \ldots 1.0$ of the cross section in the limiting case of the de Sitter model ($\lambda_0 = 1$, $\Omega_0 = 0$). This is also indicated by the grey scale, darker values corresponding to a larger cross section

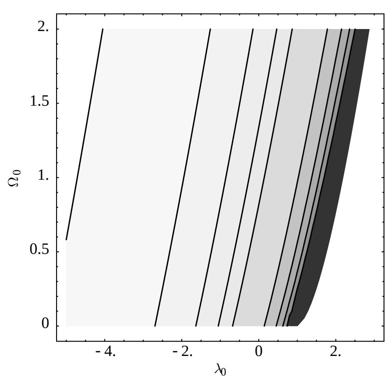

Fig. A5. Expected number of lenses. Contours, from left to right, indicate 1, 2, 3, 4, 5, 10, 15, 20 and 25 lenses. Darker values of the grey scale correspond to higher values. Cf. Cooray et al. (1999) and Cooray (1999) where the number of lenses as a function of λ_0 and Ω_0 has been calculated for the Hubble Deep Field and for CLASS

Bahcall N.A., 1998, In: Müller et al. (1998), pp. 137–146, astro-ph/9711062

Barrow J.D., 1995, Phys. Rev. D 51, 3113

Bartelmann M., Huss A., Colberg J.M., Jenkins A., Pearce F.R., 1998, A&A 330, 1

Bernardo J.M., Smith A.F.M., 1994, Bayesian Theory. Wiley, New York

Browne I.W.A., Jackson N.J., Augusto P., et al., 1998, In: Observational Cosmology with the new Radio Surveys. Kluwer Academic Publishers, Dordrecht, pp. 323–32

Carlberg R.G., 1998, In: Thanh & Giraud-Heraud (1998), astro-ph/9804329

Carlberg R.G., Yee H.K.C., Ellingson E., et al., 1998a, In: Thanh & Giraud-Heraud (1998), astro-ph/9804312

Carlberg R.G., Yee H.K.C., Lin H., et al., 1998b, In: Müller et al. (1998), pp. 119–126, astro-ph/9711272

Carlberg R.G., Yee H.K.C., Morris S.L., et al., 1998c, Phil. Trans. R. Soc. Lond. A, in press, astro-ph/9805131

Carroll S.M., Press W.H., Turner E.L., 1992, ARA&A 30, 499

Chaboyer B., Demarque P., Kernan P.J., Krauss L.M., 1998, ApJ 494, 96

Cheng Y.C.N., Krauss L.M., 1999, MNRAS, submitted, astro-ph/9810393

Coles P., Ellis G.F.R., 1994, Nat 370, 609

Coles P., Ellis G.F.R., 1997, Is the Universe Open or Closed? No. 7, In: Cambridge Lecture Notes in Physics. Cambridge University Press, Cambridge

Collins II G.W., 1997, Comments Astrophys. 18, 353

Cooray A.R., 1999, A&A 342, 353

Cooray A.R., Quashnock J.M., Miller M.C., 1999, ApJ 511, 1

da Costa L.N., Nusser A., Freudling W., et al., 1998, MNRAS 299, 425, 11Sep.

Crampton D., McClure R.D., Fletcher J.M., 1992, ApJ 392, 23

Czoske O., 1995, Die kosmologischen Parameter Ω_M und Ω_Λ. Eine Übersicht über Bestimmungsmethoden und Ergebnisse. Master's thesis, Universität Hamburg

Daly R.A., Guerra E.J., Wan L., 1998, In: Thanh & Giraud-Heraud (1998), astro-ph/9803265

Eisenstein D.J., Hu W., Tegmark M., 1998a, ApJ 504, L57

Eisenstein D.J., Hu W., Tegmark M., 1998b, ApJ, in press, astro-ph/9807130

Falco E., Kochanek C.S., Muñoz J.A., 1998, ApJ 494, 47

Fan X., Bahcall N., Cen R., 1997, ApJ 490, L123

Favati P., Lotti G., Romani F., 1991a, ACM Trans. Math. Softw. 17, 207

Favati P., Lotti G., Romani F., 1991b, ACM Trans. Math. Softw. 17, 218

Feige B., 1992, Astron. Nachr. 313, 139

Franx M., van Dokkum P., Illingworth G.D., Kelson D.D., Tran K.V., 1998, In: D'Odorico S., Fontana A., Giallongo E. (eds.), The Young Universe: Galaxy Formation and Evolution at Intermediate and High Redshift. Astronomical Society of the Pacific, vol. 146 of ASP Conference Series, p. 142

Fukugita M., Futamase T., Kasai M., 1990, MNRAS 246, 24

Fukugita M., Futamase K., Kasai M., Turner E.L., 1992, ApJ 393, 3

Gott III J.R., Gunn J.E., Schramm D.N., Tinsley B., 1974, ApJ 194, 543

Gott III J.R., Park M.G., Lee H.M., 1989, ApJ 338, 1

Guerra E.J., Daly R.A., Wan L., 1998, ApJ, submitted, astro-ph/9807249

Guth A.H., 1981, Phys. Rev. D 23, 347

Helbig P., Marlow D.R., Quast R., et al., 1999, A&AS 136, 1
Hinshaw G., Krauss L.M., 1987, ApJ 320, 468
Im M., Griffiths R.E., Ratnatunga K.U., 1997, ApJ 475, 457
Jaunsen A.O., Jablonski M., Pettersen B.R., Stabell R., 1995, A&A 300, 323
Kayser R., Helbig P., Schramm T., 1997, A&A 318, 680
Kochanek C.S., 1993, ApJ 419, 12
Kochanek C.S., 1996, ApJ 466, 638 (K96)
Kochanek C.S., Falco E.E., Schild R., 1995, ApJ 452, 109
Kochanek C.S., Falco E.E., Impey C., et al., 1997, http://cfa-www.harvard.edu/glensdata/
Krauss L.M., 1998, ApJ 501, 461
Lineweaver C.H., 1998, ApJ 505, L69
Maoz D., Bahcall J.N., Schneider D.P., et al., 1993, ApJ 409, 128
Martel H., Shapiro P.R., Weinberg S., 1998, ApJ 492, 29
Matravers D.R., Ellis G.F.R., Stoeger W.R., 1995, QJRAS 36, 29
Müller V., Gottlöber S., Mücket J.P., Wambsganß J. (eds.), 1998, Large Scale Structure: Tracks and Traces. Proceedings of the 12th Potsdam Cosmology Workshop, Potsdam Cosmology Workshops, Singapore, World Scientific
Myers S.T., Rusin D., Marlow D., et al., 1999, in preparation
Ostriker J.P., Steinhardt P.J., 1995, Nat 377, 600
Park M.G., Gott III J.R., 1997, ApJ 489, 476
Peebles P.J.E., 1993, Principles of Physical Cosmology. Princeton University Press, Princeton
Penrose R., 1989, In: Fenyves E.J. (ed.), Fourteenth Texas Symposium on Relativistic Astrophysics, New York Academy of Sciences, New York, vol. 571, pp. 249–264
Perlmutter S., Aldering G., Valle M.D., et al., 1998, Nat 391, 51
Riess A.G., Filippenko A.V., Challis P., et al., 1998, AJ 116, 1009
Schmidt B.P., Suntzeff N.B., Phillips M.M., et al., 1998, ApJ 507, 46
Schneider P., Ehlers J., Falco E.E., 1992, Gravitational Lenses. Springer-Verlag, Heidelberg
Tegmark M., Eisenstein D.J., Hu W., 1998a, In: Thanh & Giraud-Heraud (1998), astro-ph/9804168
Tegmark M., Eisenstein D.J., Hu W., Kron R.G., 1998b, ApJ, submitted, astro-ph/9805117
Thanh J.T., Giraud-Heraud Y. (eds.), 1998, Fundamental Parameters in Cosmology. Proceedings of the XXXIIIrd Rencontres de Moriond, Paris, Éditions Frontiers
Turner E.L., 1990, ApJ 365, L43
Turner E.L., Ostriker J.P., Gott III J.R., 1984, ApJ 284, 1
Turner M.S., 1996, In: Zichichi A. (ed.) Vacuum and Vacua: The Physics of Nothing. World Scientific, Singapore, p. 50
Turok N., Hawking S.W., 1998, Phys. Lett. B 432, 271
Veron-Cetty M.P., Veron P., 1996, ESO Sci. Rep. 17, 1
Webster M., Bridle S.L., Hobson M.P., et al., 1998, ApJ
White M., 1998, ApJ 506, 495
Yee H.K.C., Filippenko A.V., Tang D.H., 1993, AJ 105, 7